PERSISTENT STAGNATION POINTS AND TURBULENT CLUSTERING OF INERTIAL PARTICLES

J.C. Vassilicos[1], L. Chen[1], S. Goto[2] and D. Osborne[1]
[1] Department of Aeronautics, Imperial College London, SW7 2AZ, UK
[2] Department of Mechanical Engineering, Kyoto University, 606-8501, Japan

ABSTRACT

This is a progress report which includes some speculations as well as solid results concerning, in particular, the correlation between the clustering of inertial particles and the clustering of peristent stagnation points in statistically isotropic and homogeneous turbulent fluid flow.

1. INTRODUCTION

In many environmental, geophysical and industrial processes, inertial particles or droplets interact with turbulent flows to generate complex dispersion patterns and concentration fluctuations which can, via an agglomeration process, lead to precipitation in clouds and powders in the chemical and pharmaceutical industries. Fluctuations in particle concentrations are also responsible for large variations in the efficiency of various industrial processes and characterise air pollution in cities and elsewhere.

Here, we consider small aerosols or droplets (e.g. cloud droplets) in gases or small inertial particles in water subjected to linear Stokes drag and gravity. The particles/droplets are assumed spherical with a radius smaller than the smallest length-scale of the turbulence and a density much larger than that of the ambient fluid. The equation of motion of such particles is well approximated by $\frac{d}{dt}\mathbf{v} = \frac{1}{\tau_p}[\mathbf{u}(\mathbf{x_p},t) - \mathbf{v}(\mathbf{x_p},t)] + \mathbf{g}$ where $\mathbf{v}(\mathbf{x_p},t)$ is the velocity of the particle/droplet at its position $\mathbf{x_p}(t)$ at time t, $\mathbf{u}(\mathbf{x},t)$ is the fluid velocity field, $\mathbf{g}$ is the gravitational acceleration and τ_p is the particle relaxation time. We also assume that the particles do not significantly affect the fluid turbulence. A central concern in this paper is inertial particle clustering.

We simulate 2D inverse cascading turbulent velocity fields $\mathbf{u}(\mathbf{x},t)$ by Direct Numerical Simulation (DNS) following the method detailed in Goto & Vassilicos (2004) which gives a well-defined $-5/3$ energy spectrum. We also simulate 2D and 3D turbulent velocity fields by Kinematic Simulation (Fung & Vassilicos 1998, Osborne *et al* 2005). The emphasis is on high Reynolds number turbulence with well-defined power-law energy spectra, which is why we are concentrating on KS and 2D DNS. Recent results on inertial particle clustering obtained with 3D DNS have been reported by Collins & Keswani (2004). Instead of Reynolds numbers, we will be refering to outer- to inner-length scale ratios L/η where L is the integral length scale in our DNS but the length-scale corresponding to the smallest wavenumber in our KS and η is the small-scale forcing length-scale in our DNS but the length-scale corresponding to the small-scale end of the power-law energy spectrum in our KS. The corresponding outer- to inner-time scale ratio is T/τ_η. Inertial particles are characterised by their Stokes number $St = \tau_p/\tau_\eta$.

2. BRIEF DETAILS OF SIMULATIONS

Full accounts of our simulations can be found in the papers referenced in the previous paragraph. Here we just state that we are experimenting with 2D DNS turbulence that has a well-defined $k^{-\frac{5}{3}}$ energy specrum and $L/\eta = 30$ ($T/\tau_\eta = 25$) by using 4096^2 grid points; and that our KS velocity fields have power-law energy spectra $E(k) \sim k^{-p}$ in the range of wavenumbers $2\pi/L$ to $2\pi/\eta$ and no energy outside this range; $p = 5/3$ in all 2D KS fields considered and various values of p between 1 and 2 are tried in our 3D KS fields. The time dependence of the KS velocity fields is determined via the frequencies $\omega(k) = \lambda\sqrt{k^3 E(k)}$ where λ is a dimensionless parameter controlling the intensity of the time dependence of the fluid velocities. $L/\eta = 10^3$ (except when a dependence on L/η is sought) and, when $p = 5/3$, $T/\tau_\eta = O(100)$.

In all our 2D simulations and most of our 3D simulations, $\mathbf{g} = \mathbf{0}$. Some cases with non-zero gravity for 3D KS are reported at the end.

3. THE STOKES NUMBER AS LOW-PASS FILTER

Our DNS visualisations show that inertial particle position fields starting from initial uniformity develop well-defined near-empty spaces as time progresses (see figure 1). The locations of these near-empty spaces at given integration times are the same for different Stokes numbers and are characterised by high enstrophy values (e.g. see Crowe *et al* 1996). The sizes of these empty spaces increase with Stokes number until τ_p becomes comparable to T at which value of St these sizes saturate, with some signs of decreasing as St grows above T/τ_η. This visual observation can be quantified in terms of the coarse-grained enstrophy ω_c^2 averaged over all particle trajectories, $< \omega_c^2 >_p$ compared to its Eulerian average over space, $< \omega_c^2 >$ (see figure 2). The coarse-graining of the fluid velocity field is effected in wavenumber space by a sharp cut-off low-pass filter with cut-off wavenumber k_c. For each Stokes number, the ratio $< \omega_c^2 >_p \; / \; < \omega_c^2 >$ depends on k_c and has a minimum at $k_c = k_p$ where, for $1 \leq St \leq T/\tau_\eta$, k_p scales as $k_p\eta \sim St^{-3/2}$. This scaling is a consequence of the low-pass filtering effect of the particle relaxation time, i.e. the only wavenumbers which affect the particle motion are those smaller than k_p, where $\tau_p \sim (k_p^3 E(k_p))^{-1/2}$ (Tchen 1947). The effect of this filtering on the demixing of inertial particles, which is here measured by values of $< \omega_c^2 >_p \; / < \omega_c^2 >$ smaller than 1, is characterised by the length-scale $2\pi/k_p$ which we take to be a measure of the size of near-empty regions.

However, as St decreases further below 1, the previous paragraph does not explain what it is that these near-empty spaces and their sizes are determined by.

4. CLUSTERING AT STOKES NUMBERS SMALLER THAN 1

In approximate agreement with the 3D DNS of Collins & Keswani (2004), we find $< \omega^2 >_p / < \mathbf{s}^2 >_p \approx 1$ for $0.1 < St < 1$ in our 2D DNS (ω and $\mathbf{s}$ are the vorticity and the strain rate tensor respectively). If there is a dependence on L/η, we are unable to see it in our DNS (and we have actually run DNS cases with less grid points and smaller values of L/η than stated in section 2). However, in our 2D KS, $< \omega^2 >_p / < \mathbf{s}^2 >_p$ increases towards 2 as L/η increases towards high values, irrespective of the values of $St < 1$ and λ (see figure 3). This value 2 might suggest spatial uniformity because, in homogeneous turbulence, $< \omega^2 > / < \mathbf{s}^2 >= 2$. However, such uniformity is not observed in 2D KS visualisations (see figure 4) when λ is small enough, even at our highest values of L/η, though it is observed when $\lambda \gg 1$. This raises the issue of the persistence of turbulent eddies, controlled by λ in KS, and the impact of this persistence on particle clustering. Before addressing this issue, we briefly discuss particle compressibility.

Following Falkovich & Pumir (2004), we note that for $St \leq 0.3$, $\mathbf{v} \approx \mathbf{u} - \tau_p \mathbf{a}$ where $\mathbf{a}$ is the fluid acceleration field. Hence, the particle compressibility $\nabla \cdot \mathbf{v} \approx -\tau_p \nabla \cdot \mathbf{a} = -\tau_p(\mathbf{s}^2 - \frac{1}{2}\omega^2)$. Averaging over particle trajectories, $< \nabla \cdot \mathbf{v} >_p \approx -\tau_p (< \mathbf{s}^2 >_p - \frac{1}{2} < \omega^2 >_p)$. Our 2D KS results suggest that, in the limit $L/\eta \to \infty$, $< \nabla \cdot \mathbf{v} >_p = 0$, whereas our 2D DNS results, if they are extrapolated to mean that $< \omega^2 >_p \approx < \mathbf{s}^2 >_p$ and $< \omega^2 >_p / < \omega^2 >= 1/2$ independently of Reynolds number, imply that $\tau_\eta < \nabla \cdot \mathbf{v} >_p \sim -St$. The absolute value of the particle compressibility is an inverse time-scale τ_c which might be interpreted to be the time-scale required for the formation of near-empty spaces in the spatial distribution of inertial particles. It might be interpreted that these near-empty spaces grow within a time-scale $\tau_c \sim \tau_\eta / St$ to a size of order η (we provide evidence in section 6 for this size η) when $St \leq 1$ but that they grow to a certain size $2\pi/k_p$ defined by the relaxation time's filtering action when $St > 1$. We are currently running 2D DNS and 2D KS time-marching visualisations to validate or invalidate this interpretation. It might be worth noting here that we find $< \omega^2 >_p / < \mathbf{s}^2 >_p \approx 2$ both in 2D DNS and 2D KS when $St > 1$ in all cases of L/η and λ that we tried, even though near-empty regions are observed in all DNS cases and all KS cases except those where λ is too large.

The 2D KS results are in disagreement with elements of this picture as figures 3 and 4 testify but also highlight the importance of persistence of turbulence "eddies". The disagreements between our 2D KS and our 2D DNS are probably due either to the lack of explicit sweeping of small eddies by large ones in the modelling of KS or by the relatively modest values of L/η in DNS (or both). We do not know the answer to this question at this stage, but we do provide some elements for partially addressing it in section 6.

5. PERSISTENT STAGNATION POINTS

"Eddies" are an undefined concept, so here we focus attention on the stagnation points of the fluid velocity field $\mathbf{u}(\mathbf{x}, t)$, of the fluid acceleration field $\mathbf{a}(\mathbf{x}, t)$. In this, we follow the approach of Fung & Vassilicos (1998), Davila & Vassilicos (2003), Goto & Vassilicos (2004), Goto *et al* (2005) and Osborne *et al* (2005) who showed that velocity stagnation points do impact on turbulent pair diffusion by virtue of the strong curvature of streamlines in their vicinity as they turn out to be persistent enough in time in a statistical sense which they define. Here we discuss how the statistics of persistent stagnation points can also impact on particle clustering.

The number-density of zero-acceleration points scales as $(L/\eta)^d$ ($d = 2, 3$ for 2D and 3D respectively) whereas the number-density of zero-velocity points (irrespective of frame of reference) scales as $(L/\eta)^{D_s}$ where $p + 2D_s/d = 3$ (Davila & Vassilicos 2003, Goto & Vassilicos 2004). There is therefore many more zero-acceleration points than zero-velocity points and Goto *et al* (2005) have argued that, typically, zero-velocity points in the frame of reference where the mean fluid flow vanishes, tend to become nonmoving zero-acceleration points. The persistence of these points is partly reflected in that, as a consequence, $\frac{\partial}{\partial t}\mathbf{u} = 0$ at these points in that frame. Furthermore, Osborne *et al* (2005) present an argument showing that these points are long lived as their average life-time scales with the integral time scale. The remaining zero-acceleration points are not zero-velocity points.

For $St \leq 0.3$, $\mathbf{v} \approx \mathbf{u} - \tau_p \mathbf{a}$ and $\frac{d}{dt}\mathbf{v} = \frac{1}{\tau_p}(\mathbf{u} - \mathbf{v})$, so that persistent zero-acceleration zero-velocity points are also points where particle velocities and particle accelerations typically vanish. We might therefore expect these points to be "sticky" in the sense that particles will cluster in their vicinity. Furthermore, the clustering of inertial particles might, to some extent, reflect the clustering of these points. We address this dual clustering issue in the following section.

6. PAIR CORRELATION FUNCTIONS IN 2D DNS AND 2D KS TURBULENCE

Generalised fractal dimensions of the spatial distributions of inertial particles turn out to be equal to 2 in all our 2D turbulence simulations for all orders of generalised fractal dimensions (we tried up to order 128) (see Hentschel & Procaccia 1983 for the definition of generalised fractal dimensions). The reason is that the near-empty spaces contain enough particles, even if they are extremely dilute, for the fractal dimensions of their spatial distribution to be taking space-filling values. Clearly, a different measure of clustering is required. Here we use pair correlation functions which are simply related to the radial distribution function (Sundaram & Collins 1997) and the clustering index which is popular in analyses of observational data of atmospheric clouds (Kostinski & Jameson 2000, Kostinski & Shaw 2001, Shaw *et al* 2002). The use of the pair correlation function is based on the correlation fluctuation theorem (Landau & Lifshitz 1980). This theorem states that if a grid of grid-spacing l is superimposed on a spatial distribution of points, then the average pair correlation function $\overline{m}(l) \equiv \frac{1}{l}\int_0^l m(r)dr$ is given by

$$\overline{m}(l) = \frac{< (\delta N)^2 >_l}{< N >_l^2} - \frac{1}{< N >_l}$$

where N is the number of points in each box, $< N >_l$ the average number of points over all boxes and $< (\delta N)^2 >_l = < (N - < N >)^2 >_l$ (where the average is taken over all boxes of size l). To educe average pair correlation functions of spatial distributions of inertial particles, zero-velocity points and zero-acceleration points from our turbulence simulations we use this theorem and effectively calculate the right hand side of the above equation which is the clustering index divided by $< N >_l$. This right hand side is zero for Poisson spatial dis-

tributions and can be shown to scale as l^{-I} for homogeneous-fractal spatial distributions (see Hentschel & Procaccia 1983 for a definition of homogeneous fractals) with $I = d - D_0$ where D_0 is the lowest order generalised fractal dimension (i.e. the usual box-counting fractal dimension). It is important to point out that a power law $\overline{m}(l) \sim l^{-I}$ is an indication of a multiple size structure of near-empty regions except when $I = 1$, in which case the pair correlation function $m(r)$ is a constant different from zero up to a certain length-scale (which characterises the size of near-empty regions) and equal to 0 for r larger than this length-scale. Increasing values of $\overline{m}(l)$ reflect increasing clustering.

Such a well-defined power-law is indeed observed both in 2D DNS and in 2D KS with λ small ($L/\eta = 10^3$ and $\lambda = 0.5$) when $St \leq 1$, with I tending to 1 as $St \to 0$ in both cases. The exponent I decreases as St increases towards 1 but decreases only by about 10% for St smaller than about 0.5, and so remains close to 1. For all intents and purposes, $m(r) \approx 0$ for $r \geq \eta$ and $m(r) \neq 0$ for $r < \eta$ in our DNS (and also in KS as some preliminary results seem to indicate) when $St < O(1)$ (see figure 5), hence supporting the view (see section 4) that the near-empty spaces grow to be of order η in size. We also note that $\overline{m}(l)$ and $m(r)$ calculated for snapshots taken at the same time increase as St tends to 1 from below (i.e from values smaller than 1) both in KS and in DNS ($m(r)$ is obtained from differentiation of $\overline{m}(l)$). This observation is in agreement with the claim made in section 4 for our 2D DNS turbulence that near-empty spaces of size η form within a time-scale $\tau_c \sim \tau_\eta/St$, i.e. that it takes longer for these near-empty spaces to reach their final size η when St is smaller. We are currently checking this claim in DNS and KS. Even though this qualitative observation is also valid in KS, it is a bit harder to explain because in KS $< \nabla \cdot \mathbf{v} >_p \to 0$ as $L/\eta \to \infty$ and τ_c^{-1} cannot be defined as $| < \nabla \cdot \mathbf{v} >_p |$. We are currently investigating the behaviour of $(< \nabla \cdot \mathbf{v} >_p)^2$ in KS as a function of St, L/η and λ.

As St increases above 1 towards T/τ_η, the values of $\overline{m}(l)$ continuously decrease both in KS and DNS and there is again a critical size r_* above which $m(r) \approx 0$ (i.e. for $r \geq r_*$) which is larger than η and continuously increases with St, generating the impression that r_* is determined by the low-pass filter wavenumber k_p discussed in section 3. However, we have not yet verified this hypothesis quantitatively.

Maximum clustering in the sense of maximum values of $\overline{m}(l)$ (but also directly observed on plots of inertial particle distributions in space) occurs at $St \approx 1$. The time scale τ_* required to generate near-empty spaces of size r_* is $\tau_c \sim \tau_\eta/St$ for St sufficiently smaller than 1 (in which case $r_* = \eta$) but is $(k_p^3 E(k_p))^{-1/2} \sim \tau_\eta St$ for St larger than 1 (in which case $r_* = 2\pi/k_p$). Hence, this time scale τ_* is minimal at $St \approx 1$ which might explain the observation that clustering is maximal at $St \approx 1$.

In figure 6 we plot the pair correlation functions $m(r)$ of zero-acceleration points and zero-velocity points (in the frame where the mean fluid flow is zero) obtained from our DNS (similar calculations are currently being carried out for KS. Zero-velocity points are more clustered than zero-acceleration points as the pair correlation functions (and therefore also $\overline{m}(l)$) of the zero-velocity points are larger by one order of magnitude than those of zero-acceleration points. Following the suggestions of section 5, we plot the pair correlation function of inertial particles for a case of near-maximum clustering ($St = 1.9$) obtained at a time significantly larger than T and find that it coincides quite closely with the pair correlation function of zero-acceleration points (see figure 7). In figures 8 we visualise side by side the spatial distribution of zero-acceleration points and the spatial distribution of inertial particles to reveal the remarquable spatial correlation which exists between these two spatial distributions over a range of spatial resolutions. All the results mentioned in this paragraph have been obtained for DNS; the corresponding KS calculations are currently under way.

How do these results square with the suggestion of section 5 that, in the limit $L/\eta \to \infty$, inertial particles "stick" around persistent zero-velocity zero-acceleration points? To answer this question, we now argue that for large enough values of L/η, inertial particles stick around zero-acceleration points and move with them, but that as L/η increases towards very high values, some of these zero-acceleration points tend to identify with zero-velocity points and as a result move slower and slower in the frame where the mean fluid flow is zero, thus becoming increasingly persistent in that frame. The persistence of these points becomes an essential ingredient in the clustering of inertial particles in the limit $L/\eta \to \infty$.

Our argument, which we now sketch, is valid for $St \leq 0.3$, but our numerical results indicate that its conclusions may be valid more widely. Generalising the approach of Goto *et al* (2005) and Osborne *et al* (2005) to zero-acceleration points, we define these points $\mathbf{s}_a(t)$ by $\mathbf{a}(\mathbf{s}_a(t), t) = 0$, their velocity by $\mathbf{V}_a \equiv \frac{d}{dt}\mathbf{s}_a(t)$ and write

$$\frac{D}{Dt}\mathbf{a} + (\mathbf{V}_a - \mathbf{u}) \cdot \nabla \mathbf{u} = 0$$

at these points, where $\frac{D}{Dt}$ is the Lagrangian time derivative following fluid elements and $\mathbf{u}$ is the fluid velocity at $\mathbf{s}_a(t)$ at time t. Assuming that $(\mathbf{V}_a - \mathbf{u})$ and $\nabla \mathbf{u}$ are statistically uncorrelated, we deduce that

$$< |\mathbf{V}_a - \mathbf{u}|^2 >^{1/2} \sim < |\frac{D}{Dt}\mathbf{a}|^2 >^{1/2} / \tau_\eta.$$

where we reasonably assume Kolmogorov scaling for velocity gradients. Such scaling implies that $< |\frac{D}{Dt}\mathbf{a}|^2 >^{1/2} \sim (u'^3/L^2)(L/\eta)^{-1}$, where u' is the r.m.s. turbulent fluid velocity, which in turn implies

$$< (\mathbf{V}_a - \mathbf{u})^2 >^{1/2} \sim u'(L/\eta)^{-1/3}.$$

The important consequence is that $< (\mathbf{V}_a - \mathbf{u})^2 >^{1/2} / u' \to 0$ as $L/\eta \to \infty$, meaning that in the limit of high Reynolds numbers, zero-acceleration points move with their local fluid velocity $\mathbf{u}$. This conclusion can be seen as a quantitative formulation of the Tennekes sweeping hypothesis which states that energy containing turbulent eddies advect small-sale dissipative turbulent eddies (see Goto *et al* 2005 and references therein).

For $St \leq 0.3$, $\mathbf{v} \approx \mathbf{u} - \tau_p \mathbf{a}$ and $\frac{d}{dt}\mathbf{v} = \frac{1}{\tau_p}(\mathbf{u} - \mathbf{v})$ so that, when $L/\eta \gg 1$, an inertial particle at a zero-acceleration point moves, on average, *with* this zero-acceleration point because they both move, statistically, with the same velocity $\mathbf{u}$. Furthermore, the acceleration $\frac{d}{dt}\mathbf{v}$ of an inertial particle at a zero-acceleration point is zero, thus reducing the particle's ability to escape from the zero-acceleration point. This conclusion goes some way in explaining why the spatial clusterings of zero-acceleration points and of inertial particles are

so well correlated in our DNS calculations where $L/\eta = 30$. As the Reynolds number of the turbulence increases we expect inertial particle clustering to increasinly correlate with a subset of zero-acceleration points, namely the subset of persistent zero-velocity zero-acceleration points, and we present some evidence to this effect in the following section.

Let us end this section by noting that the validity of the scaling relations leading to these conclusions, in particular $< |\mathbf{V}_a - \mathbf{u}|^2 >^{1/2} \sim < |\frac{D}{Dt}\mathbf{a}|^2 >^{1/2} / \tau_\eta$, is currently being investigated by well-resolved 2D DNS and KS. Preliminary results not included here support our conclusions.

7. PAIR CORRELATION FUNCTIONS IN 3D KS TURBULENCE

Values of the average pair correlation function of inertial particles turn out to be orders of magnitude larger in 3D KS with small values of λ (we have experimented with (small) $\lambda = 0.5$ and (large) $\lambda = 5$) than in our 2D turbulent flows. Furthermore, they exibit very well-defined power laws of the grid-spacing l over a wide range of scale (note that here $L/\eta = 10^3$), particularly for $St \leq 1$ (see Figure 9). In the case $St \leq 1$, we have checked that this power law is the same for all St tried between 0.1 and 1.0 and for both cases $Fr \equiv gL/u'^2 = 0$ and 9.8. We have also checked that our algorithms give uniformly vanishing average pair correlation functions when $St = 0$, but have not yet investigated what happens at extremely small values of St, i.e. between 0 and 0.1.

As St increases above 1 and towards T/τ_η (and keeping $\lambda = 0.5$), the average pair correlation function of inertial particles decreases for all grid-spacings l but does so whilst apparently keeping a sufficiently well-defined power law of l with an exponent that is a decreasing function of St; in fact this exponent tends to 0 as $St \to T/\tau_\eta$ (see Figure 10). When λ is given large values these properties of the average pair corelation of inertial particles are lost and $\overline{m}_p(l)$ collapses to very small values (the subscript p indicates inertial particles). This dramatic dependence on λ illustrates the importance that the persistence of the fluid turbulence has for the particle clustering.

To find whether, in the case $\lambda = 0.5$ of 3D KS turbulence with persistent properties, there is a correlation between the clustering of inertial particles and the clustering of zero-velocity points in the frame where the mean fluid flow is zero (as predicted in sections 5 and 6), we plot the average pair correlation functions of zero-velocity points, $\overline{m}_s(l)$, and of inertial particles with $St = 1$ for different values of the exponent p of the energy spectrum (see Figures 11 & 12). The result is $\overline{m}_s(l) \sim l^{I_s}$ and $\overline{m}_p(l) \sim l^{I_p}$ with $I_p - p$ and $I_s - p$ both equal to a constant as the exponent p varies. This indicates a clear correlation which relates to the fact that as p increases from 1 to 2, the total number of stagnation points per unit volume *decreases* as $n_s \sim (L/\eta)^{(9-3p)/2}$ (see Davila & Vassilicos 2003) from $n_s \sim (L/\eta)^3$ to $n_s \sim (L/\eta)^{3/2}$. Less number density of stagnation points is not inconsistent with more clustering of stagnation point but is definitely consistent, according to our arguments in the previous sections, with more clustering of inertial particles. Indeed as p increases from 1 to 2, $\overline{m}_p(l)$ increases too across the l-range, thus indicating increased clustering.

8. CONCLUSION

We have argued that zero-acceleration points and inertial particles are correlated and cluster together at least for small enough Stokes number and high enough values of L/η, and we have presented preliminary results from turbulence simulations supporting this view. We have also argued that in the limit of very high Reynolds numbers, the clustering of inertial particles is determined by persistent zero-velocity zero-acceleration points and have presented supporting results from 3D KS which also suggest that the average pair correlation exponents I_p (of inertial particles for small enough St) and I_s (of zero-velocity points) are close to each other irrespective of the exponent p characterising the energy spectrum $E(k) \sim k^{-p}$, i.e. $I_p - I_s$ is independent of p.

REFERENCES

Collins, L.R. & Keswani, A., 2004, "Reynolds number scaling of particle clustering in turbulent aerosols," *New J. Phys.* **6**, 119.

Crowe, C.T., Troutt, T.R. & Chung, J.N., 1996, "Numerical models for two-phase turbulent flows," *Ann. Rev. Fluid Mech.*, **28**, 11-43.

Davila, J. & Vassilicos, J.C., 2003, "Richardson's pair diffusion and the stagnation point structure of turbulence," *Phys. Rev. Lett.*, **91**, 144501.

Falkovich, G. & Pumir, A., 2004, "Intermittent distribution of heavy particles in a turbulent flow," *Phys. Fluids*, **16**, L47.

Fung, J.C.H. & Vassilicos, J.C., 1998, "Two-particle dispersion in turbulent-like flows," *Phys. Rev. E*, **57**, 1677.

Goto, S., Osborne, D.R., Vassilicos, J.C. & Haigh, J.D., 2005, "Acceleration statistics as measures of statistical persistence of streamlines in isotropic turbulence," *Phys. Rev. E*, **71**, 015301

Goto, S. & Vassilicos, J.C., 2004 , "Particle pair diffusion and persistent streamline topology in two-dimensional turbulence," *New J. Phys.*, **6**, 65.

Hentschel, H.G.E. & Procaccia, I., 1983, "The infinite number of dimensions of probabilistic fractals and their strange attractors," *Physica D*, **8**, 435.

Kostinski, A.B. & Jameson, A.R. 2000, "On the spatial distribution of cloud particles," *J. Atmospheric Sc.*, **57**, 901.

Kostinski, A.B. & Shaw, R.A., 2001, "Scale-dependent droplet clustering in turbulent clouds," *J. Fluid Mech.* **434**, 389.

Landau, L.D. & Lifshitz, E.M., 1980, Statistical Physics, Pergamon Press.

Osborne, D.R., Vassilicos, J.C. & Haigh, J.D., 2005, "Fundamentals of pair diffusion in kinematic simulations of turbulence," *Phys. Fluids*, (submitted).

Shaw, R.A., Kostinski, A.B. & Larsen, M.L., 2002, "Towards quantifying droplet clustering in clouds," *Quarterly Journal of the Royal Meteorological Society*, **128**, 1043.

Sundaram, S. & Collins, L.R., 1997, "Collision statistics in an isotropic particle-laden turbulent suspension," *J. Fluid Mech.* **335**, 75.

Tchen, C.M., 1947, "Mean values and correlation problems connected with the motion of small particles suspended in turbulent fluid," Doctoral Dissertation, Delft, Holland.

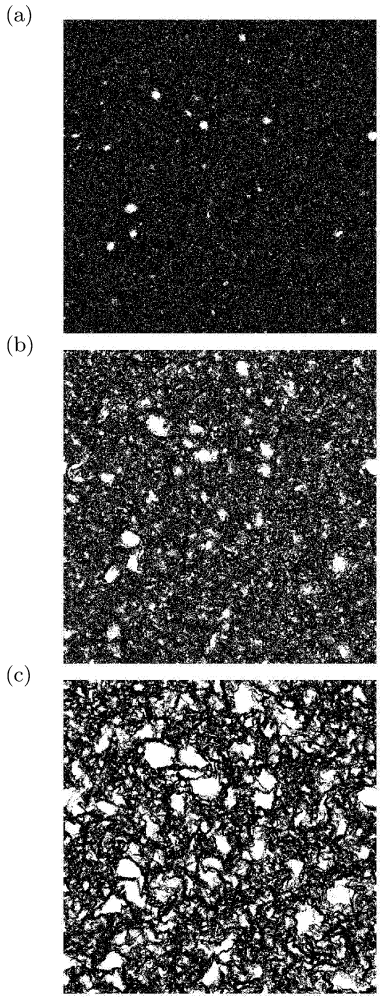

Figure 1: Particle distributions in 2D DNS turbulence for three different Stokes numbers; (a) $St = 0.1$, (b) 0.8 and (c) 6.4. The entire periodic domain is shown.

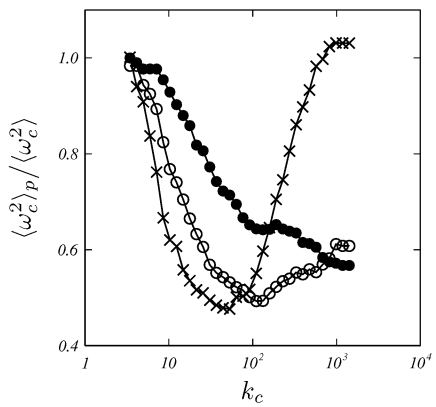

Figure 2: Average of the coarse-grained vorticity with cut-off k_c at the postion of inertial particles (•, $St = 0.1$; ∘, 0.8; ×, 6.4.)

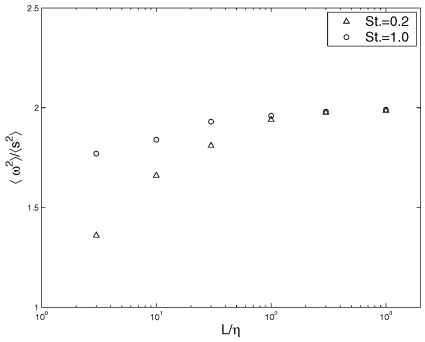

Figure 3: $< \omega^2 >_p / < \mathbf{s}^2 >_p$ for KS with $\lambda = 0.5$. Larger values of λ lead to faster convergence towards 2.

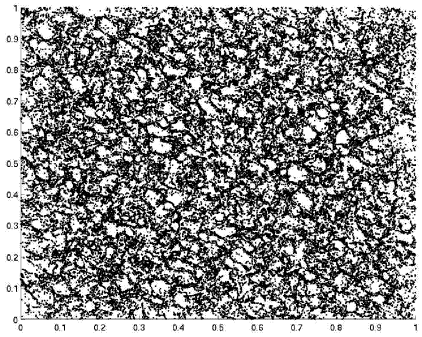

Figure 4: Particle distributions in 2D KS turbulent field. $St = 1.0$, $L/\eta = 1000$, $\lambda = 0.5$, Box size is $10L$.

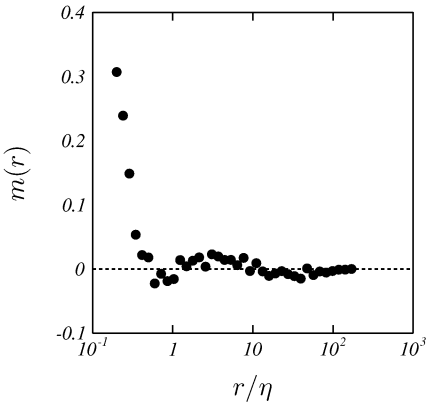

Figure 5: Correlation function $m(r)$ of inertial particles ($St = 0.4$). 2D DNS.

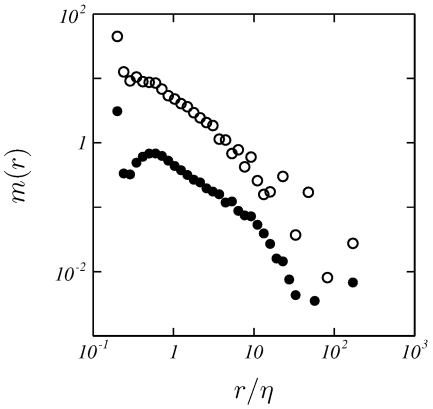

Figure 6: Correlation function $m(r)$ for zero-acceleration points (•) and for zero-velocity points (○). 2D DNS.

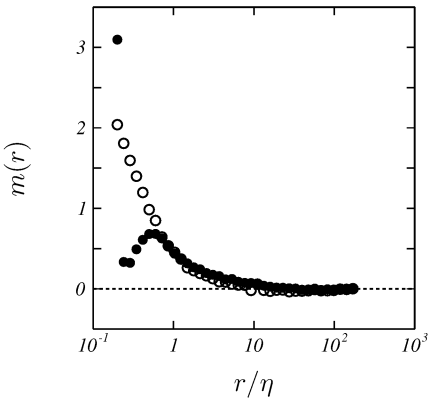

Figure 7: Correlation function $m(r)$ for inertial particles ($St = 1.9$, ○) and zero-acceleration points (•). 2D DNS.

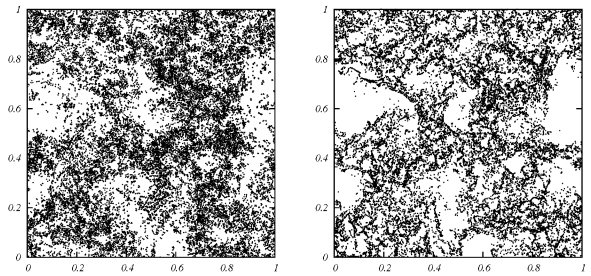

Figure 8: Distribution of (a) inertial particles ($St = 1.6$) and (b) zero-acceleration points. 2D DNS. The figure size equals about four integral length scales.

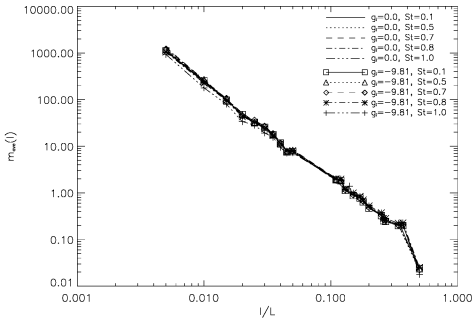

Figure 9: Average pair correlation functions for inertial particles in 3D KS with $-5/3$ spectrum, $\lambda = 0.5$.

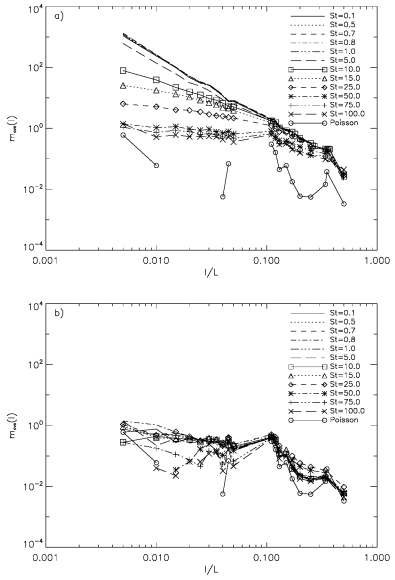

Figure 10: Average pair correlation functions for inertial particles in 3D KS with $-5/3$ spectrum: a) $\lambda = 0.5$, b) $\lambda = 5$. $Fr = 0$. A comparison is included with results from a Poisson disrtribution.

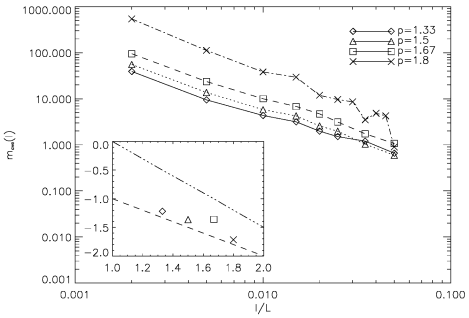

Figure 11: Average pair correlation functions for zero-velocity points in 3D KS with $\lambda = 0.5$ and various values of p. Inset depicts the exponent I_s as a function of p.

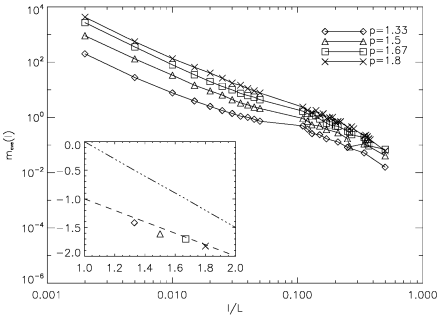

Figure 12: Average pair correlation functions for inertial particles with $St = 1$ in 3D KS with $\lambda = 0.5$ and various values of p. Inset depicts the exponent I_p as a function of p.